Desalination and Water Treatment
www.deswater.com

doi: 10.5004/dwt.2021.27160

224 (2021) 256–272
June

Experimental studies on the removal of heavy metal ion concentration using sugarcane bagasse in batch adsorption process

V. Yogeshwaran[a,*], A.K. Priya[b]

[a]*Department of Civil Engineering, Sri Krishna College of Engineering and Technology, Coimbatore – 641008, India, email: svyogi23190@gmail.com*
[b]*Department of Civil Engineering, KPR Institute of Engineering and Technology, Coimbatore – 641027, India, email: akpriy@gmail.com*

Received 16 August 2020; Accepted 18 February 2021

ABSTRACT

Removal of toxic heavy metal ion concentration (Cr, Pb, and Zn) from the aqueous solution has been investigated using sugarcane bagasse as an adsorbent. The various properties of sugarcane bagasse powder were analyzed and the Fourier transmission infrared spectra, scanning electron microscopy, and energy dispersive X-ray analysis of sugarcane bagasse powder, before and after adsorption of Cr(VI), Pb(II), and Zn(II) were also examined. Test results show that the maximum adsorption efficiency of 95.65% for Cr(VI), 87.26% for Pb(II), and 83.32% for Zn(II) were attained at the pH of 6.0, the temperature of 30°C, the contact time of 60 min, the adsorbent dosage of 2.5 g/L with 25 mg/L of metal ion concentrations. The Langmuir and Freundlich isotherm models were adopted for the batch adsorption experimental work and the results prove that the pseudo-second-order model was fitted well with kinetic data. Also, the thermodynamic study confirms that adsorption mechanism is endothermic in nature with the best possible correlations.

Keywords: Heavy metals; Adsorption; Fourier transmission infrared; Scanning electron microscopy; Energy dispersive X-ray; Thermodynamic studies; Sugarcane bagasse powder

1. Introduction

Water pollution is one of the serious issues that we are facing for many eras. Fresh clean water is the essence for major industrial activities, communities, and all living organisms. The supply of clean water without any pollutant is one of the critical challenges and many countries are doing lots of research works to find a viable solution to this problem by various techniques [1]. The water gets highly polluted in recent times due to extreme activities of industrial manufacturing and other pathogenic activities [2]. This makes the water unsuitable for drinking by changing its physical and chemical properties [3]. Pollution in water may be created by the presence of dyes, metal ions, suspended and dissolved solids, and other organic and inorganic pollutants at very high concentration levels. Among various pollutants in water, heavy metal pollution is one of the serious issues due to metal ion toxicity and accumulation and poses to be very dangerous to the surrounding environment and human beings [4]. On account of the increase in heavy metal pollution day by day, the present world faces many health issues such as cancer, respiratory problems, and other health issues (Table 1). Hence, it is necessary to reduce/remove the accumulation of heavy metal ions present in wastewater before discharging them into the water bodies. Many research works have been conducted to remove the accumulation of heavy metal ions from the wastewater [5]. The batch adsorption process was developed as a promising and innovative solution for removing metal ion concentration [6]. This process has many advantages such as low capital cost, selective metal removal, desorption with no sludge generation [7]. The adsorption process, which is an accumulation of

* Corresponding author.

atoms, ions, or gaseous molecules to the adsorbate surface by batch mode or fixed-bed column type has been long used for removal/reduction of heavy metal ions [8]. Using various adsorbate materials (both natural and industrial wastes), toxic metal ions have been removed by the adsorption process. Normally, the adsorbent material is converted into the activated carbon category for increasing the efficiency of the adsorption process [9]. Many natural adsorbents such as rice husk, neem leaves, sawdust, coconut shells rice bran, etc., were used for removing different metal ion concentrations from the aqueous medium [10].

Sugarcane bagasse powder is a type of organic material that has been used for removing heavy metal ion contamination from aqueous solutions in this study. These are the fractions of biomass which is produced after the extraction of sugarcane juice. Sugarcane bagasse is the heterogeneous fiber residue and around 30–34 tons can be produced from 100 tons of sugarcane in the factory process and these fibers are renewable and are used to produce biofuel and enzymes [11]. The decomposition period of sugarcane bagasse is around 45–60 d and these are eco-friendly materials that are produced around 80 MMT (million metric tonnes) annually in India [12]. Handling and disposal of sugarcane bagasse are one of the huge tasks and it consumes more time and money. Hence it is decided to use the sugarcane bagasse powder in water treatment, particularly for heavy metal ion removal. Many research works have been conducted to remove the heavy metal ions present in the aqueous solutions using sugarcane bagasse. From Table 2, it was observed that the sugarcane bagasse has the ability to remove various heavy metal ions from an aqueous environment. In this experimental study, the adsorption efficiency of heavy metal ions (Cr, Pb, and Zn) has been investigated using sugarcane bagasse powder in activated carbon form.

2. Materials and methods

2.1. Preparation of adsorbent

Sugarcane bagasse was collected and washed with de-ionized water and then dehydrated for 24 h at 60°C to eliminate tannins and other solvent organic complexes. The stock was cooled, purified, and washed several times with distilled water and eventually dried to 60°C. To boost stability, the bagasse was treated by 1% formaldehyde at a ratio of 1:4 (sugarcane bagasse: formaldehyde, weight/volume). The water is boiled for 6 h at 100°C and dried in an oven at 105°C for about 24 h. Table 3 represents the physical properties of sugarcane bagasse powder.

2.2. Pore distribution and Brunauer–Emmett–Teller surface area

The pore diameter, Brunauer–Emmett–Teller (BET) surface area, volume of micropore, and mesopore of SBP were obtained using adsorption–desorption isotherm process by nitrogen at –196°C temperature. Fig. 1 shows the nitrogen adsorption–desorption rate of SBP adsorbent and their characteristics are presented in Table 4. From Fig. 1, both the isotherms were seen to follow type II; which means that the SBP contains micropores and mesopores. The micropores are represented in the first part of the isotherm plot and mesopores are represented in the second part at high relative pressure, due to the adsorption of multilayers [17]. The BET surface area of SBP was about 558 m^2/g which is smaller than other commercial activated carbons with a pore volume of 0.275 cm^3/g. The BET surface area of 0.5 m^2/g with a total pore volume of 2.70×10^{-3} cm^3/g of white yam has been reported by Li et al. [18] for Cd^{2+} ion adsorption. Another study has been reported by Jing et al. [19] for activated

Table 1
Trace elements that may pose health hazards

S. No	Element	Atomic No.	Sources	Health effects
(1)	Vanadium	23	Petroleum, chemicals and catalysts, steel, and other alloys	Probably no hazard at current levels
(2)	Chromium	24	Metal electroplating	A micronutrient to plant, chromates carcinogenic
(3)	Manganese	25	Mining and industrial wastes	Relatively non-toxic, and micro nutrient
(4)	Nickel	28	Fuel oil, coal, tobacco smoke, chemicals and catalysts, steel, and non-ferrous alloys	Lung cancer
(5)	Copper	29	Waste pipes, algae control, and industrial smoke	Possible liver damage with prolonged exposure, toxic to plants
(6)	Zinc	30	Metal electroplating, mining, and industrial smoke	Possible lung effects, low toxicity in solution
(7)	Arsenic	33	Coal, petroleum, detergents, pesticides	Arsenic poisoning
(8)	Selenium	34	Coal, sulfur	May cause dental caries, carcinogenic to rats, essential to mammals in low doses
(9)	Cadmium	48	Coal, Zinc mining, water mains and pipes, tobacco smoke	Cardiovascular disease and hypertension in human suspects interferes with zinc and copper metabolism
(10)	Lead	82	Auto exhaust, paints, and water through the lead joint of pipes	Brain damage, convulsions, behavioral disorder, and fatality

Table 2
List of research work conducted for metal ion removal using sugarcane bagasse

S. No.	Type of heavy metal ion	Adsorption efficiency	Concentration of heavy metal ions (mg/L)	Optimum pH	Adsorbent dose	Contact time (min)	Reference
(1)	Cr^{6+}, Pb^{2+}, and Zn^{2+}	95.65%, 87.26%, and 83.32%	25	6.0	2.5 g/L	60	In this study
(2)	Fe^{2+}	95.11%	10.87	6.0	0.2 g	100	[13]
(3)	Cu^{2+}, Ni^{2+}, and Pb^{2+}	66.4%, 90%, and 99.9%	25	4.0	7.5 g/L	70	[14]
(4)	Cu^{2+}, Ni^{2+}, and Pb^{2+}	268, 700, and 320 mg/g	100	3.0	5 g/L	180	[15]
(5)	Cr^{6+} and Zn^{2+}	98.84% and 94.67%	30	4.0	1.5 g	30	[11]
(6)	Cu^{2+}	94.4%	5	5.0	2 g	120	[16]
(7)	Cd^{2+}	90.9 mg/g	200	6.5	1.5 g	60	[5]

Table 3
Physical properties of treated sugarcane bagasse powder

S. No	Physical parameters	Sugarcane bagasse powder
(1)	Specific gravity	0.53
(2)	Bulk density (g/cc)	0.37
(3)	Porosity (%)	84
(4)	Surface area (m^2/g)	27
(5)	Average particle size	0.6–0.425 μm
(6)	Moisture content (%)	39.2
(7)	Loss in ignition	93.22 (w/w %)
(8)	Al_2O_3	2.2 (w/w %)
(9)	SiO_2	1.05 (w/w %)

Table 4
Pore characteristics of SBP adsorbent

Parameter	Value
BET surface area, m^2/g	558
Pore volume, cm^3/g	0.275
Micropore volume, cm^3/g	0.181
Mesopore volume, cm^3/g	0.075
Micropore area, m^2/g	385
Average pore diameter, Nm	0.8–2.4

carbon derived from bamboo and observed the BET surface area of 2,024 m^2/g with a pore volume of 0.999 cm^3/g.

2.3. Preparation of metal ion solutions

100 mg of potassium di-chromate ($K_2Cr_2O_7$), lead sulfate ($PbSO_4$), and zinc chloride ($ZnCl_2$) has been mixed with 1 L of double distilled water separately and the stock solutions were prepared. To obtain various design concentrations, the prepared water was diluted with double distilled water. Using 0.1 M of HCL, pH adjustments were carried out for the entire studies.

2.4. Batch adsorption studies

Adsorption of heavy metal ions onto the adsorbent has been conducted through batch mode by adjusting the parameters such as pH, contact time, adsorbent dose, metal ion concentrations, and temperature. The impact of the removal of heavy metal ions onto the adsorbent were examined with 50 mg/L of metal ion concentration, 100 mL of solution with pH of 2.0–7.0 at 30°C, for the equilibrium period of 60 min. By varying the adsorbent dosage from 0.5 to 2.5 g/L, the impact was analysed. The conical flasks were kept on the rotary shaker, shaken for 60 min for ensuring attainment of equilibrium. The impact of contact time has been investigated by varying the time from 10 to 120 min. The total amount of metal ions adsorbed onto the adsorbent was calculated at various time intervals using Eq. (1) as given below:

$$q_t = \frac{\left(C_0 - C_t\right)V}{m} \text{ mg/g} \tag{1}$$

where q_t is the amount of metal ion adsorbed onto the adsorbent at any time "t" (mg/g), C_t is the concentration of batch adsorption processes.

The metal ion solutions were centrifuged for 5 min and residual concentration of metal ions was found out using atomic adsorption spectroscopy (AAS). Each analysis was repeated twice and the results were taken as an average of these values. The percentage removal of metal ions can be calculated by using the data obtained from batch studies. The mass balance relationship was obtained from Eq. (2):

$$\%\text{Removal} = \left(\frac{C_0 - C_e}{C_0}\right) \times 100 \tag{2}$$

where C_0 is the initial concentration of the metal ion solution (mg/L); C_e is the equilibrium concentration of the metal ion solution (mg/L); V is the volume of the metal ion solution; m is the mass of the adsorbent used.

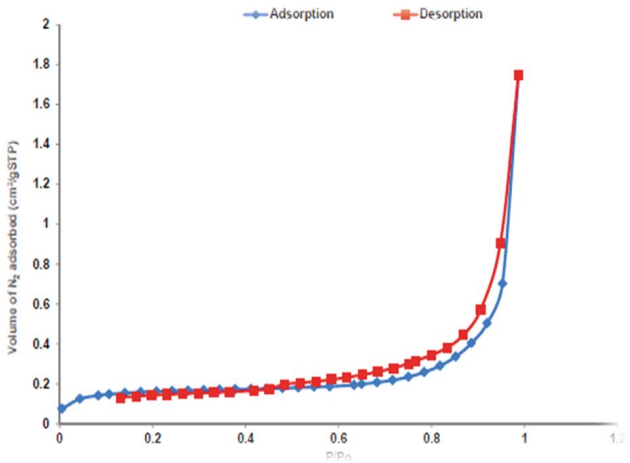

Fig. 1. Nitrogen adsorption–desorption isotherm.

2.5. Kinetic studies

For equilibrium studies, the initial concentration of metal ion solution has been varied from 25 to 150 mg/L with 2 g/L of SBP dose at the pH of 6.0 in 100 mL solutions. The temperature was fixed at 30°C and solutions were shaken up to 60 min at a speed of 120 rpm in a rotary shaker. Then the supernatant was taken for analysis using filter paper. The amount of metal ions adsorbed onto the adsorbent at equilibrium, q_e (mg/g) was calculated by Eq. (3):

$$q_e = \frac{\left(C_0 - C_e\right)V}{m} \text{ mg/g} \tag{3}$$

where C_0 and C_e are the initial and equilibrium metal ion concentrations respectively (mg/L); V is the volume of the metal ion solution; m is the mass of the adsorbent used.

Table 5 represents the various types of kinetic model studies used for this experimental work along with their constants and equations.

2.6. Temperature and thermodynamic studies

Batch adsorption experiments were performed at different temperatures of 15°C, 30°C, 45°C, and 60°C with the sugarcane bagasse powder for fixed initial metal ion concentration, adsorbent dose, and pH. To confirm whether the adsorption process is exothermic or endothermic in nature, thermodynamic parameters such as Gibbs free energy ($\Delta G°$), enthalpy change ($\Delta H°$), and entropy change ($\Delta S°$), were calculated from the experimental data obtained from batch studies. The thermodynamic parameters, such as Gibbs free energy ($\Delta G°$), enthalpy change ($\Delta H°$), and entropy change ($\Delta S°$) were calculated from Eqs. (4)–(6) as follows:

$$K_c = \frac{C_{\text{Ae}}}{C_e} \tag{4}$$

$$\Delta G° = -RT \ln K_c \tag{5}$$

$$\log K_c = \frac{\Delta S°}{2.303R} - \frac{\Delta H°}{2.303RT} \tag{6}$$

where K_c is the equilibrium constant; C_e is the equilibrium of the metal ion concentration in solution (mg/L); C_{Ae} is the amount of metal ions adsorbed on the adsorbent per litre solution at equilibrium (mg/L); R is the gas constant – 8.314 J/mol K; T is the temperature.

2.7. Adsorption isotherm studies

2.7.1. Langmuir isotherm model

It is based mainly on few assumptions such as monolayer adsorption, and that adsorbate binding to the surface of adsorbent happens predominantly by chemical reactions, and all sites have an equivalent preference for adsorbate [25]. This isotherm follows few assumptions such as, all the process are homogeneous, only one adsorbate is used and these adsorbate molecules react with only one active site, in the adsorbate species no interactions are formed and the surface phase is monolayer [26].

The Langmuir isotherm equation can be expressed as in Eq. (7).

$$\frac{C_e}{q_e} = \frac{1}{Kq_{\max}} + \frac{C_e}{q_{\max}} \tag{7}$$

where C_e is the equilibrium concentration of the adsorbate solution; q_e is the amount of adsorbate adsorbed per g; K and $q_{\max}$ is the Langmuir constants related to the adsorption capacity and intensity.

2.7.2. Freundlich isotherm model

This isotherm model allows the multi-layer adsorption on the adsorbent surface [27]. The Freundlich isotherm equation is expressed in Eq. (8):

$$\ln q_e = \ln k_f + \frac{1}{n} \ln C_e \tag{8}$$

where q_e is the amount of adsorbate adsorbed per g; n is the energy of intensity or adsorption; k_f is the Freundlich constant related to adsorption capacity; C_e is the equilibrium concentration of the adsorbate solution.

2.8. Interaction of heavy metal ions

The interaction of heavy metal ions onto the adsorbent in the adsorption process is of great significance for investigation, because of the presence of various metal ions in the effluent [28]. The impact of interaction with heavy metal ions on the adsorption of Cr(VI), Pb(II), and Zn(II) were tested by varying the initial metal ion concentrations from 25 to 150 mg/L.

3. Results and discussion

3.1. Scanning electron microscopy and energy dispersive X-ray analysis

The scanning electron microscopy(SEM) and energy dispersive X-ray (EDX) images of sugarcane bagasse powder and Cr(VI), Pb(II), and Zn(II) metal ions – adsorbed

Table 5
Different types of kinetic plots and their constants

Type of kinetic model	Kinetic equation	Kinetic constants	References
Pseudo-first-order	$\log\left(q_e - q\right) = \log q_e - \frac{k}{2.303}t$	k and q_e	[20]
Pseudo-second-order	$\frac{t}{q} = \frac{1}{h} + \frac{1}{q_e}t$	k, q_e, and h	[21]
Elovich	$q_t = \frac{1}{b}\ln\left(1 + abt\right)$	a and b	[22]
Boyd	$B = \frac{\Pi^2 D_i}{r^2}$	B and D_i	[23]
Intra-particle diffusion	$q_t = k_p t^{1/2} + C$	k_p and C	[24]

sugarcane bagasse powder are shown in Figs. 2a and b. From Fig. 2a, it was observed that the surface was porous and the material was irregular in shape. From this, the surface morphology of the adsorbent can be identified for the adsorption of metal ions. Fig. 2b shows the loaded metal ions of Cr(VI), Pb(II), and Zn(II) onto the sugarcane bagasse powder. At the time of adsorption process, permeable surface on the adsorbent (sugarcane bagasse) gets occupied by metal ions. On account of the presence of functional groups in bagasse surface inner walls, the metal ions were adsorbed onto them [29]. From the above surface morphology study, it becomes evident that sugarcane bagasse powder has been loaded with metal ions and can be absorbed in the internal walls of the adsorbent surface.

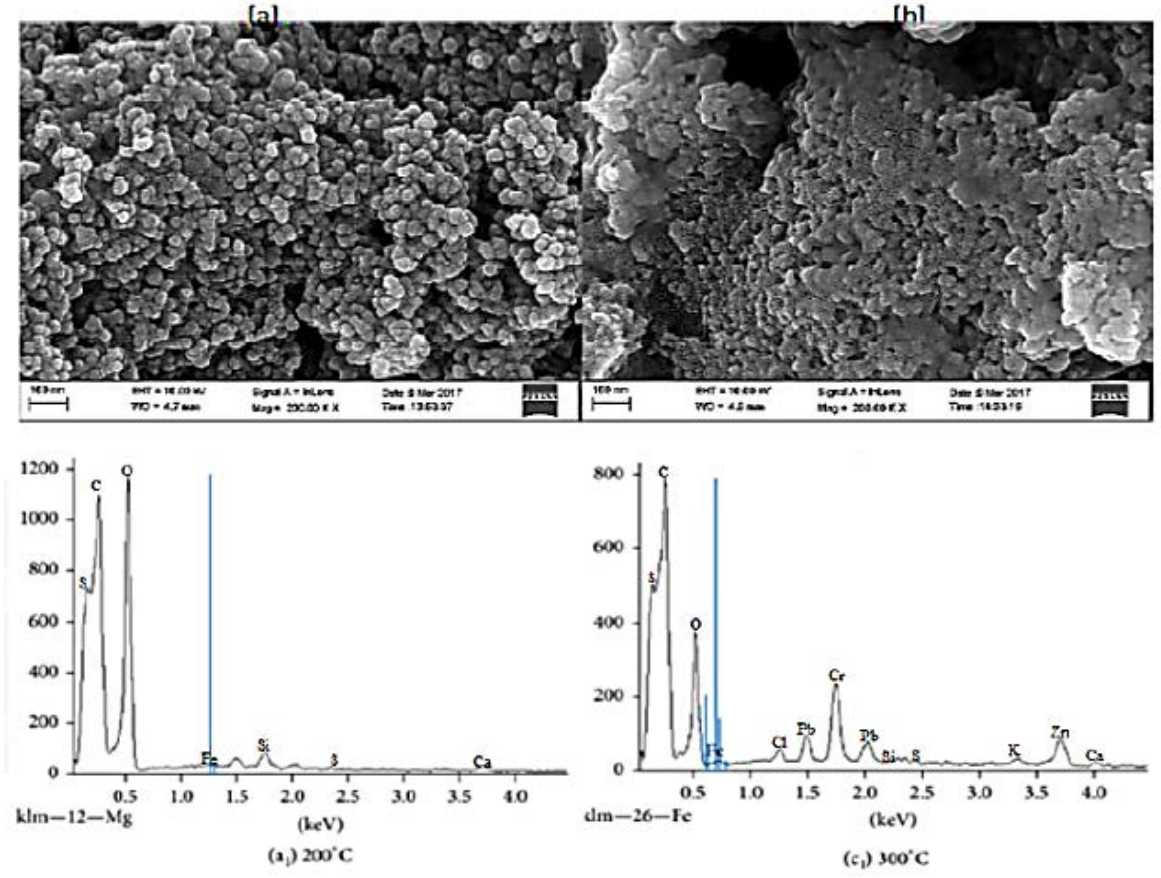

Fig. 2. (a and b) SEM/EDX images of raw and metal ion loaded adsorbent.

The EDX image of raw and metal ion loaded adsorbent has been shown in Figs. 2a and b and it confirm the presence of chromium, lead, and zinc ions after the adsorption process. Apart from chromium, lead, and zinc ions adsorbed, the raw adsorbent such as carbon, oxygen, and sulfur are seen in the EDX image of metal ion loaded adsorbent. Referring to Figs. 2a and b, additional metal elements/components were identified such as calcium, silica, and chlorine. Due to the acid treatment of sugarcane bagasse powder, the concentrated sulphuric acid reacts with hydroxyl groups present in the adsorbent and forms sulphuric esters as a non-ionic functional group, which may complex cations [30]. Hence it is concluded that the treatment with sulfuric acid solution protonates the charged sites and does not destroy any significant functional groups of raw adsorbent [31].

3.2. Fourier transmission infrared studies

The Fourier transmission infrared (FT-IR) analysis of sugarcane bagasse and Cr(VI), Pb(II), and Zn(II) metal ion loaded sugarcane bagasse is shown in Fig. 3. From Fig. 3, it is clear that there is a presence of –OH and $–CH_2$ groups (3,420 and 2,860 cm^{-1}) in the high energy region. The band range of 1,000–1,800 cm^{-1} represents the vibrations of aqueous solutions such as water (1,620 cm^{-1}), around 1,600–1,460 cm^{-1} for aromatic vibrations, and in the range of 1,380 and 1,400 cm^{-1} for $–CH_2$ bending vibrations and 1,080 cm^{-1} for C–O vibrations. If the aromatic vibrations are due to C–H bending, the peak goes below 1,000 cm^{-1} [32]. The spectrum of sugarcane bagasse and metal ions (Cr, Pb, and Zn) loaded sugarcane bagasse indicates the aromatic ring vibrations and –OH stretching because of low frequencies [33]. Further, the $–CH_2$ stretching vibrations will disappear at 2,860 cm^{-1}. From sugarcane bagasse and metal ion-loaded sugarcane bagasse FT-IR spectra, it was observed that there is a presence of active sites in the adsorbent for the adsorption process.

3.3. Impact of solution pH on metal ion adsorption

The impact of solution's pH with the removal of metal ions such as Cr(VI), Pb(II), and Zn(II) were investigated using sugarcane bagasse as an adsorbent, which had a pH range of 2.0 to 7.0. This study shows that the percentage of metal ions diminishes with the rise in pH of the solution up to 6.0 and their effect reduces subsequently. The surface of the adsorbent was enclosed by hydronium ions at a lower pH level as shown in Fig. 4. The interaction between metal ions and adsorbent has been reduced due to the presence of a high positively charged adsorbent surface. When the pH is low, the surface of the adsorbent becomes less positively charged stimulating faster removal of heavy metal ions [26]. The metal ions become less stable when the pH of the solution increases and adsorption reaches equilibrium at 6.0. At higher pH values, there is a decrease in metal ion removal, which can be attributed to precipitation into their respective hydroxides. The sugarcane bagasse powder can be used as an adsorbent up to a maximum range of 93.55% for Cr(VI), 87.56% for Pb(II), and 83.27% for Zn(II) at an optimum pH.

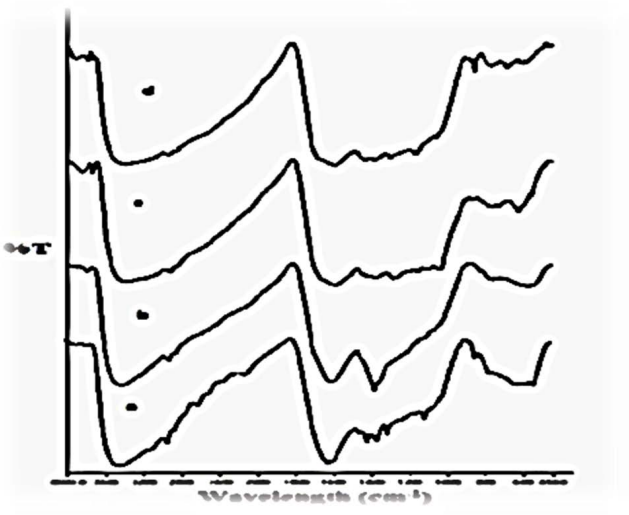

Fig. 3. FTIR spectra of (a) raw and (b–d) metal ions (Cr(VI), Pb(II), and Zn(II)) loaded adsorbent.

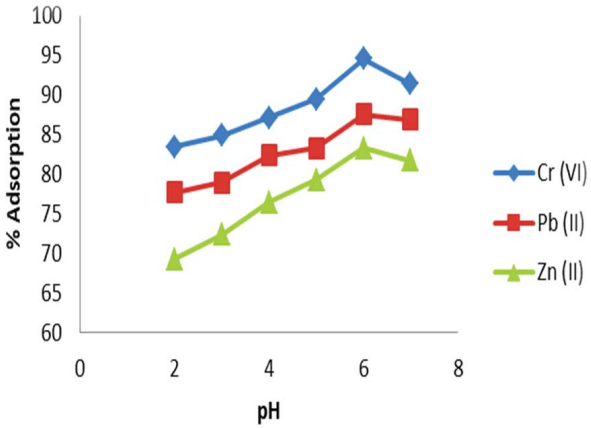

Fig. 4. Impact of pH on metal ion removal by SBP (concentration = 50 mg/L, dose = 1.5 g/L, time = 90 min, and temperature = 30°C).

3.4. Impact of adsorbent dosage on metal ion adsorption

Adsorbent dosage specifies the amount of active sites and serves as a significant criterion for the initial and final concentration of metal ions [34]. Fig. 5 indicates the influence of various dosages of sugarcane bagasse on the removal efficiency of metal ions such as Cr(VI), Pb(II), and Zn(II), respectively. The maximum range of eliminating various heavy metals was found to be 93.55% for Cr(VI), 77.7% for Pb(II), and 59.2% for Zn(II) at a dosage of 2.5 g/L. The number of available active sites in the adsorbent has been found to be proportional to the efficiency of heavy metals removal from an aqueous solution.

3.5. Impact of contact time on metal ion concentration

The impact of contact time between adsorbent particles and adsorbate is a vital parameter. Investigations were carried out by varying the concentration (25–150 mg/L)

of metal ion solution with different contact periods. The contact time was adjusted from 10 to 120 min for each adsorption study (Figs. 6a–c). During the initial stages, the removal rate of metal ions (Cr, Pb, and Zn) was found to be rapid due to the higher availability of vacant sites. In addition, heavy metal ions were adsorbed into the mesopores that get saturated [22]. After a period of 60 min, there was no significant change in metal ion removal, that is, it remains constant. This is due to repulsive forces on the solid surface between adsorbate molecules [35]. Hence, the mass transfer between the phase of solids and liquids decreases with the passage of time. Furthermore, the metal ions have to travel farther and deeper through the pores with even higher strength. This results in slowing down the adsorption during the later phases.

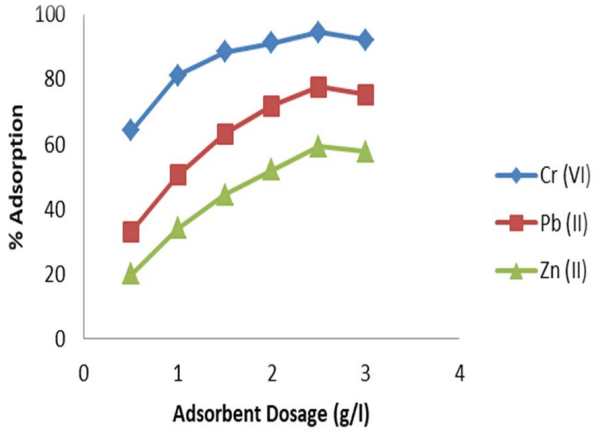

Fig. 5. Impact of adsorbent dose on metal ion removal by SBP (concentration = 50 mg/L, pH = 6.0, time = 90 min, and temperature = 30°C).

3.6. Impact of temperature on metal ion adsorption

The impact of temperature on the metal ion adsorption process is related to many thermodynamic parameters. Studies are conducted for varying temperatures (15°C–60°C) while the other parameters like adsorbate concentration, adsorbent concentration, and equilibrium time were kept constant and had values of 50 mg/L, 2.5 g/25 mL, and 60 min, respectively. The efficiency of the adsorption process gradually increased and attained a constant rate at a temperature of 45°C (optimum). Beyond this temperature, the efficiency gradually decreased due to an increase in desorption rate. Fig. 7 shows the adsorption efficiency of adsorbents in various temperature levels from 15°C to 60°C.

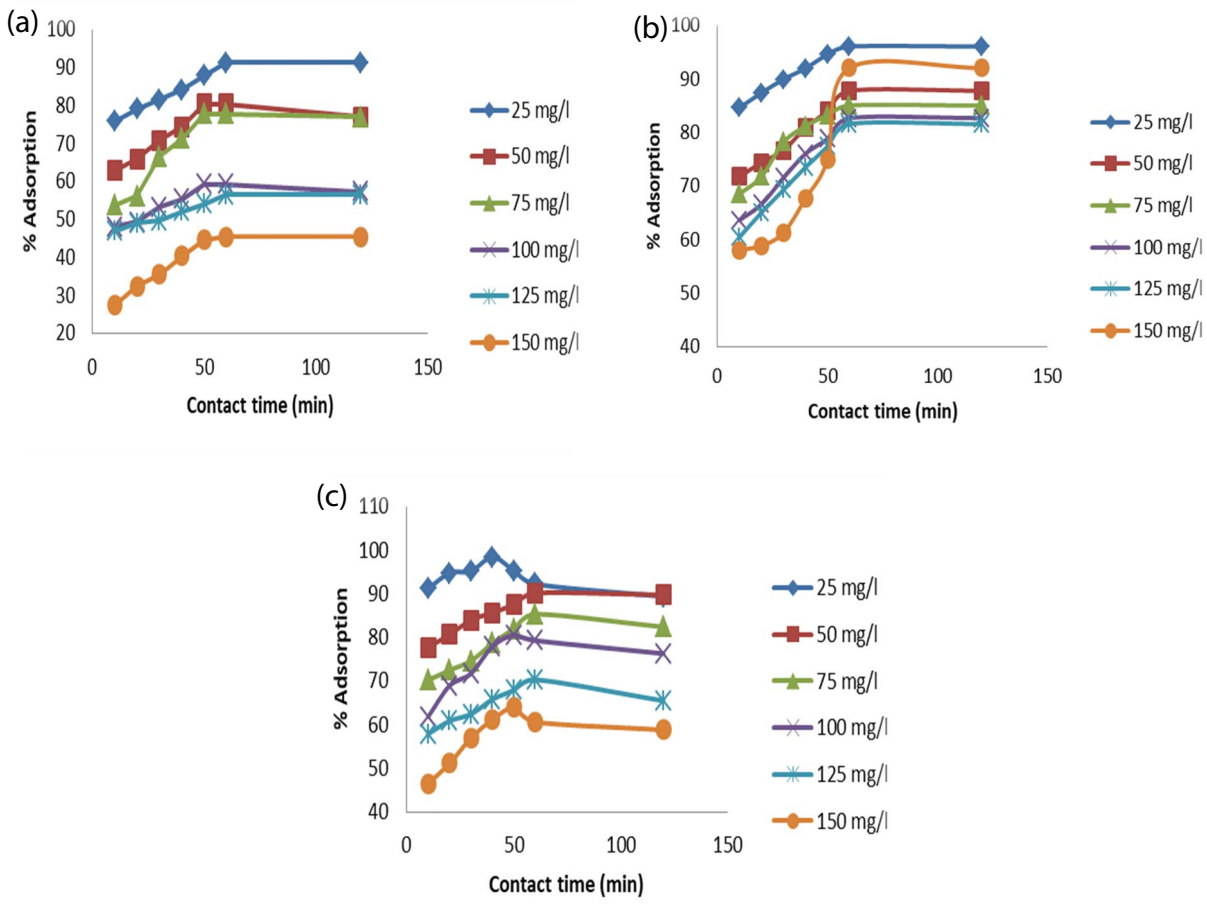

Fig. 6. (a–c) Impact of contact time on Cr(VI), Pb(II), and Zn(II) adsorption (pH 6.0, dose = 2.5 g/L, temperature = 30°C, and concentration = 25–150 mg/L).

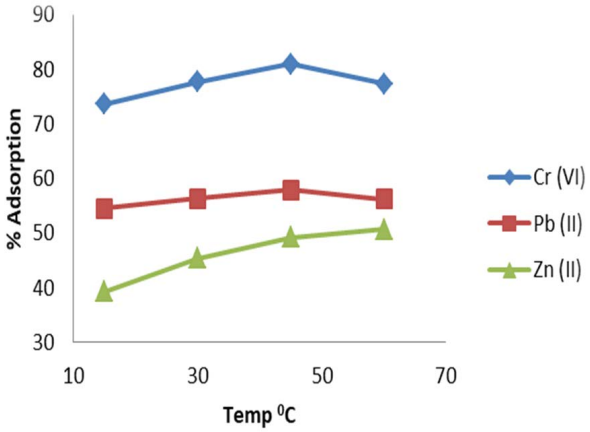

Fig. 7. Impact of temperature on metal ion adsorption (pH = 6.0, time = 60 min, concentration = 50 mg/L, and dose = 2.5 g/L).

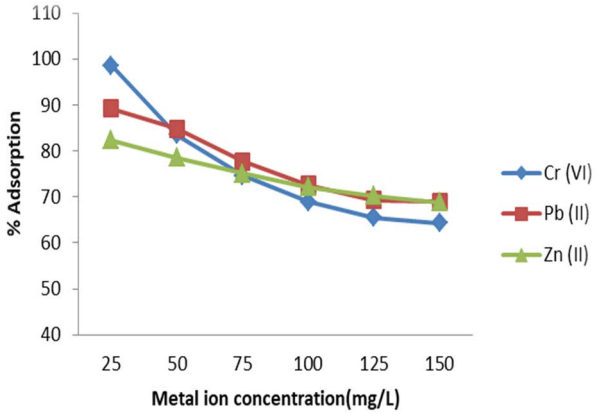

Fig. 8. Interaction of metal ions in multi-stage level (adsorbent dose = 2.0 g/L, pH = 2.0, time = 90 min, and temperature = 30°C).

3.7. Interaction of metal ions

From Fig. 8, the percentage of adsorption was gradually decreased from 98.63% to 64.26% for Cr(VI), 89.27% to 68.92% for Pb(II), and 82.39% to 68.82% for Zn(II), with an increase in metal ion concentration (25–150 mg/L). The amount of adsorption decreases uniformly with an increase in metal ion concentration indicates that adsorbent material has not reached the saturation level. Based on the above results, it was identified that the amount of adsorption shows a substantial difference between single and multi – heavy metal ions adsorbed onto sugarcane bagasse powder. Compared to Pb(II) and Zn(II), the adsorption rate of Cr(VI) is high. For 150 mg/L of multi-metal ion concentration, the sugarcane bagasse powder adsorbed 68.92% of Cr(VI) single metal ions. A similar trend has been followed for Pb(II) and Zn(II) metal ions also. Compared to multi-metal ion analysis, single metal ion adsorption provides the maximum adsorption efficiency due to the availability of a large amount of strived adsorption sites. The competitions between heavy metal ions are very much stronger in the higher concentration level of the mixed stage. The Pb(II) and Zn(II) can be replaced by Cr(VI) to be adsorbed on the surface of the adsorbent. Therefore, Cr(VI) was more competitive than Pb(II) and Zn(II). The performance of adsorbent for removal of Cr(VI) is higher due to high atomic weight and paramagnetic of metal ions, reduction potential is very high as compared to Pb(II) and Zn(II). Also, the hydration energy and ionic radius of metal ions are very low which are easier for adsorption [36,37].

3.8. Kinetic studies on metal ion adsorption

3.8.1. Pseudo-first-order kinetic model

Pseudo-first-order reaction model explains the adsorption kinetics. The plot of $\log(q_e - q)$ vs. time "t" is shown in Fig. 9 for various metal ions (Cr(VI), Pb(II), and Zn(II)). The rate constant "k" and correlation coefficient "R^2" were calculated for different metal ion concentrations (25–150 mg/L) and represented in Table 6. From those observations, it was found that the regression coefficients (R^2) are in good contract with pseudo-first-order kinetics [38].

3.8.2. Pseudo-second-order kinetic model

Pseudo-second-order kinetic model may also be relevant to the kinetics of sorption. The kinetics plots of t/q vs. t were made at different adsorbate concentrations is shown in Fig. 10 for different metal ions (Cr(VI), Pb(II), and Zn(II)). The correlation coefficients, h and k values are calculated from the plot as shown in Table 6. From the above discussion, it can be decided that the adsorption process of Cr(VI), Pb(II), and Zn(II) metal ions using sugarcane bagasse powder is best suited to pseudo-second-order kinetics study as "R^2" values matched well [39]. The findings suggested that the observed R^2 values for pseudo-first-order equation were small and the discrepancy between measured q_e and experimental q_e values was large. Hence, the pseudo-second-order model was a better choice of study for metal ion adsorption using sugarcane bagasse powder [27].

3.8.3. Elovich kinetic model

Using sugarcane bagasse powder, the kinetics of metal ion adsorption is verified with Elovich kinetic model by plotting q_t vs. $\ln(t)$ and the findings are seen in Fig. 11 for Cr(VI), Pb(II), and Zn(II) metal ions respectively with various concentrations. The Elovich kinetic constants (a and b) were estimated from the plot and are mentioned in Table 6. The obtained values of regression coefficient (R^2) from the Elovich kinetic model were lower than the values obtained from pseudo-second-order kinetic model. But, the Elovich model is used for explaining the heterogeneous adsorbents in the adsorption process [18].

3.8.4. Boyd kinetic model

B_t vs. t plots were used to check the experimental variables and their linearity. If the plots passes through the origin and are of linear type, then the intra-particle diffusion is the slowest stage in the adsorption method, and vice versa. Fig. 12 shows the metal ion adsorption of Cr(VI), Pb(II), and Zn(II) using sugarcane bagasse powder, for various concentrations, which indicates that the plots are circular but do not move into the origin [40]. It shows

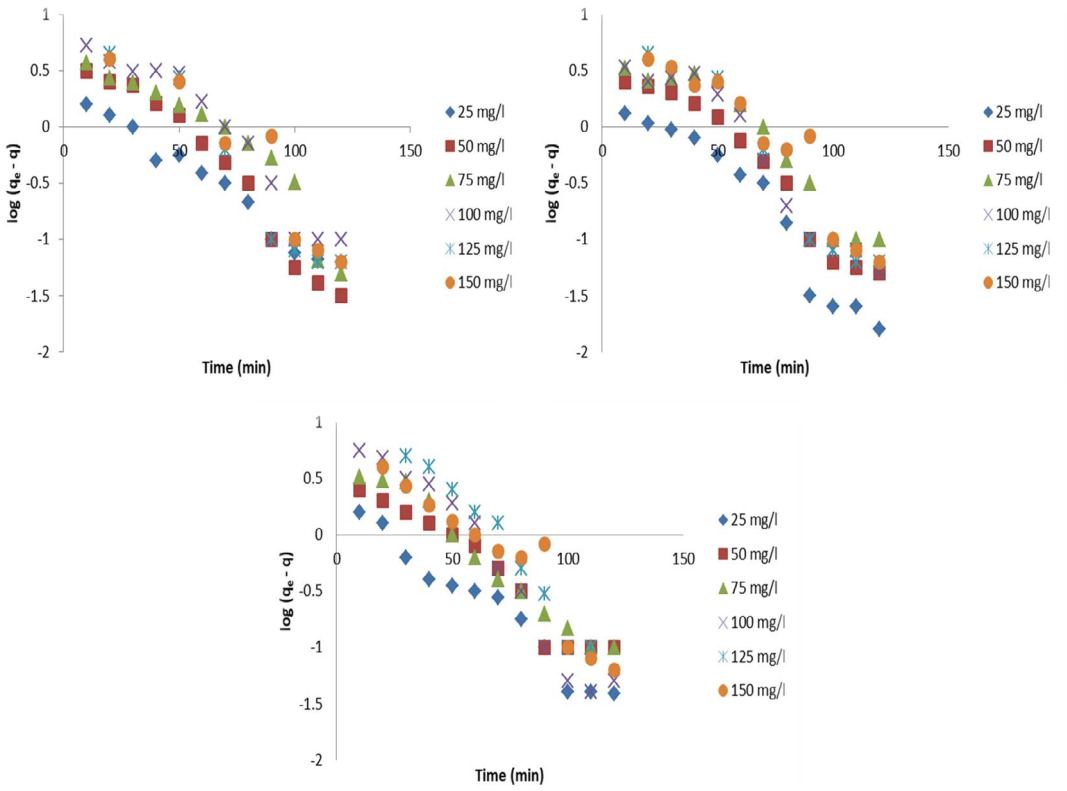

Fig. 9. Pseudo-first-order kinetic plots of Cr(VI), Pb(II), and Zn(II) metal ions.

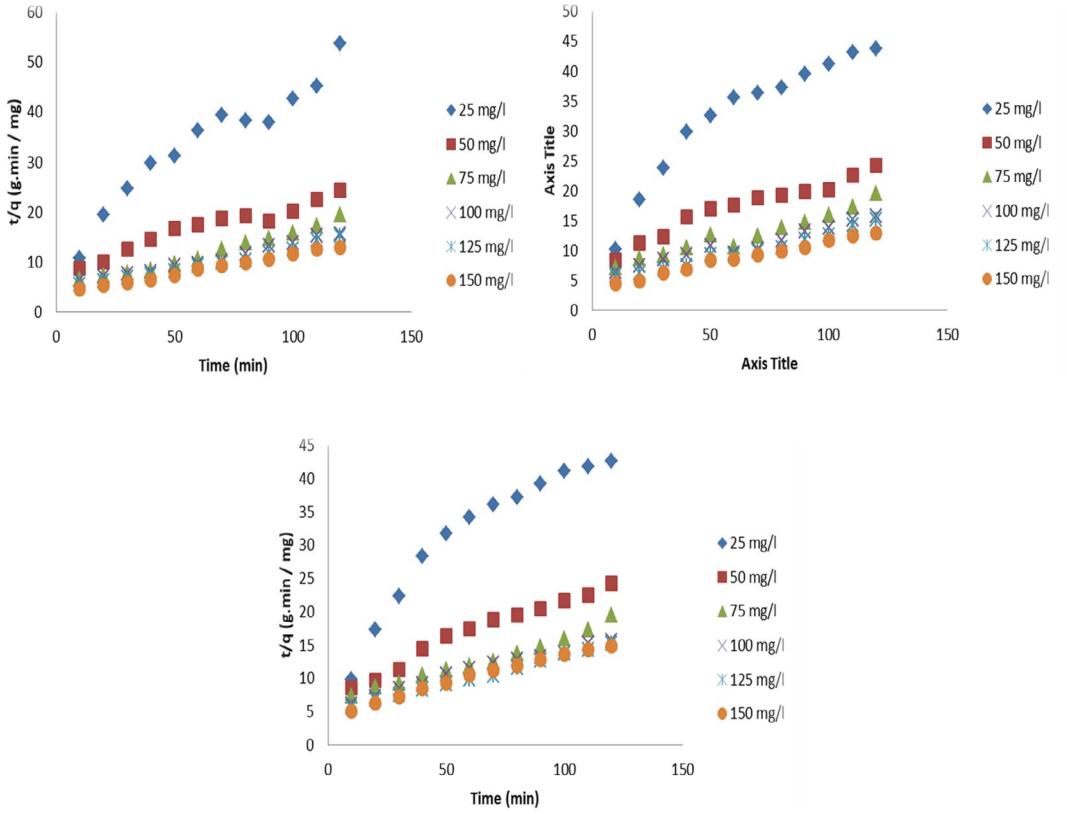

Fig. 10. Pseudo-second-order plots of Cr(VI), Pb(II), and Zn(II) metal ions.

Table 6
Kinetic constants and its parameters of different kinetic models

S. No.	Type of metal	Conc.	Pseudo-first-order			Pseudo-second-order				Elovich			Boyd			Intra-particle diffusion		
		(mg/L)	k (min^{-1})	$q_{e,cal}$ (mg/g)	R^2	k (g/mg min) × 10^{-3}	$q_{e,cal}$ (mg/g)	h (mg/g min)	R^2	a (mg/g min)	b (g/mg)	R^2	B	D_i (×10^{-3} m^2/s)	R^2	k_p (mg/g $min^{1/2}$)	C	R^2
1	Cr(VI)	25	0.034	2.640	0.950	16.690	2.150	0.100	0.960	0.244	1.550	0.940	0.034	5.472	0.915	0.197	0.410	0.950
2		50	0.043	7.020	0.930	5.730	5.190	0.180	0.980	0.988	0.740	0.930	0.044	7.340	0.973	0.399	0.580	0.950
3		75	0.041	10.000	0.930	3.340	8.300	0.220	0.980	0.978	0.550	0.920	0.043	7.621	0.963	0.517	0.600	0.980
4		100	0.039	11.360	0.940	5.070	10.750	0.260	0.980	0.948	0.440	0.950	0.039	6.856	0.914	0.783	0.540	0.990
5		125	0.048	17.470	0.920	2.000	12.910	0.290	0.970	0.977	0.350	0.920	0.049	8.725	0.982	0.804	0.370	0.930
6		150	0.045	19.430	0.930	3.120	13.820	0.300	0.960	0.934	0.260	0.920	0.045	7.452	0.952	0.856	0.320	0.960
7	Pb(II)	25	0.046	3.680	0.910	12.620	2.700	0.100	0.970	0.263	1.160	0.910	0.046	7.678	0.943	0.190	0.380	0.980
8		50	0.041	6.540	0.930	5.320	5.470	0.120	0.980	0.328	0.810	0.940	0.041	6.294	0.983	0.348	0.510	0.940
9		75	0.043	9.950	0.920	3.560	8.600	0.230	0.980	0.541	0.650	0.930	0.045	7.959	0.924	0.554	0.680	0.950
10		100	0.046	12.380	0.940	2.770	10.100	0.280	0.970	0.611	0.470	0.920	0.046	7.678	0.983	0.686	0.670	0.950
11		125	0.052	20.550	0.920	2.300	11.560	0.310	0.980	0.618	0.310	0.900	0.053	8.590	0.941	0.772	0.510	0.970
12		150	0.050	25.480	0.940	2.650	12.730	0.330	0.960	0.596	0.200	0.920	0.055	8.972	0.922	0.805	0.320	0.960
13	Zn(II)	25	0.039	2.840	0.950	15.430	2.140	0.090	0.960	0.230	1.630	0.940	0.037	6.428	0.993	0.189	0.300	0.970
14		50	0.032	6.510	0.930	5.310	5.550	0.150	0.990	0.323	0.870	0.960	0.041	6.492	0.939	0.318	0.370	0.980
15		75	0.041	10.400	0.910	3.640	7.740	0.210	0.970	0.484	0.650	0.940	0.046	7.687	0.920	0.514	0.420	0.940
16		100	0.044	13.270	0.950	2.860	9.400	0.270	0.980	0.572	0.460	0.930	0.050	8.344	0.942	0.677	0.410	0.950
17		125	0.044	18.350	0.940	1.350	12.640	0.230	0.980	0.652	0.360	0.920	0.049	8.725	0.941	0.746	0.320	0.960
18		150	0.051	23.470	0.950	1.110	15.230	0.250	0.950	0.549	0.250	0.910	0.045	8.921	0.955	0.840	0.270	0.970

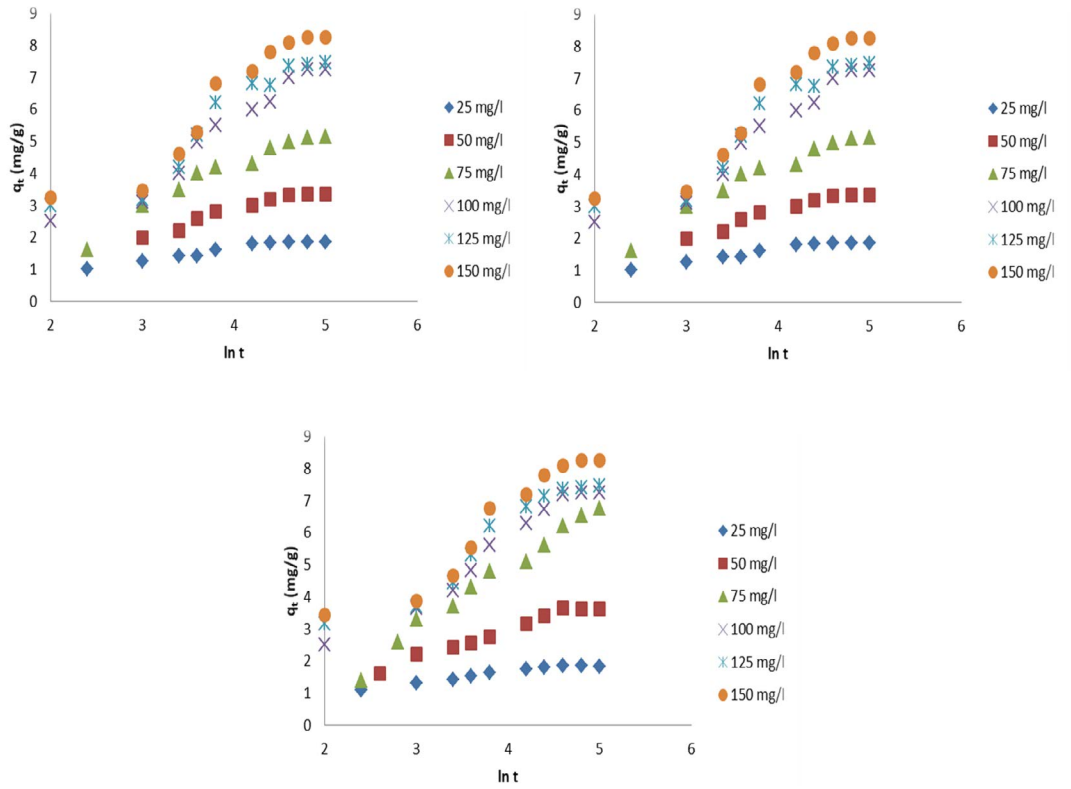

Fig. 11. Elovich kinetic plots of Cr(VI), Pb(II), and Zn(II) metal ions.

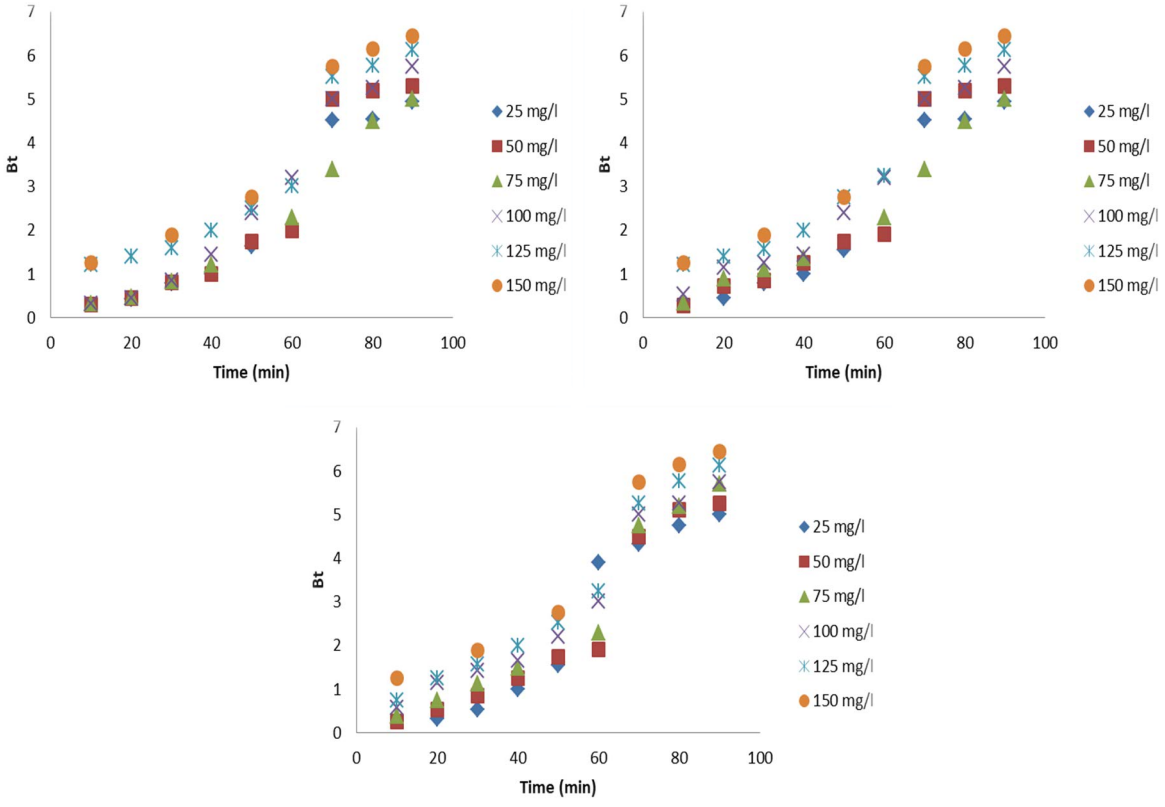

Fig. 12. Boyd kinetic plots of Cr(VI), Pb(II), and Zn(II) metal ions.

that the adsorption of metal ions to sugarcane bagasse powder is regulated by external or film diffusion [41]. The values of D_i and B were calculated from the plot and shown in Table 6 along with regression coefficient "R^2" values.

3.8.5. Intra-particle diffusion model

The plot of q_t vs. $t^{0.5}$ is shown in Fig. 13 for Cr(VI), for Pb(II) and Zn(II) metal ions, respectively, in different concentrations and the values of IPD constants (k_p, C, and R^2) were calculated (Table 6). The IPD plots pass through the origin, then metal ions adsorption to the adsorbents is regulated by intra-particle diffusion, whereas if the data display a multi-linear curve pattern, two or more phases influence the adsorption cycle [16,42]. The dual structure of the curve is characterized by the differing degrees of adsorption in the preliminary and final stages of adsorption with sugarcane bagasse powder. It may be recognized to the assumption that at the early stage, adsorption was due to diffusion effect of boundary layer and, at a later point to diffusion impact of intraparticle [40]. By referring to Fig. 13, it can be shown that the plots are linear and the mechanism is driven by film diffusion.

3.9. Adsorption isotherm studies

3.9.1. Langmuir adsorption isotherm

The Langmuir isotherm plots of C_e/q_e vs. C_e is shown in Fig. 14 for Cr(VI), Pb(II), and Zn(II) metal ions adsorption using sugarcane bagasse powder. The constants of the Langmuir isotherm study ("k," q_{max}, and R^2) were obtained from Fig. 14 and listed in Table 7 at the temperature of 30°C. From that Table 7, it was observed that the regression coefficients (R^2) are <1 for all three heavy metal ions with 100 mg/L concentrations. The reported R^2 values are between 0 and 1 for all metal ions tested with sugarcane bagasse powder, which means that the adsorption is favorable [35].

3.9.2. Freundlich adsorption isotherm

The Freundlich isotherm constants k_f and n were calculated and listed in Table 7, by referring to the plots of $\ln q_e$ vs. $\ln C_e$ (Fig. 15). The degree of non-linearity between adsorption and metal ion concentration was indicated based on the "n" values [13]. The adsorption process is in the linear stage the value of "n" equal to 1. If the value of "n" is less than1, it indicates that the process is chemically oriented and "n" value is greater than 1, it is physically oriented [14]. The Freundlich constants (k_f and n) with R^2 values were derived from the plot of $\ln q_e$ vs. $\ln C_e$ at 30°C, and are listed in Table 7. The "n" values were found to be 2.936, 2.351, and 2.062 for Cr(VI), Pb(II), and Zn (II) ions, respectively, for sugarcane bagasse powder adsorbent. Since the "n" values are greater than 1 it indicates that the metal ion adsorption follows the physical adsorption process [6]. Experimental results from the analysis of the preliminary accumulation of metal ions onto sugarcane bagasse powder surfaces are fitted with Langmuir and Freundlich adsorption isothermal models, and the plots of these models are shown in Figs. 14 and 15. From the obtained R^2 values, the best fit of the adsorption isotherms

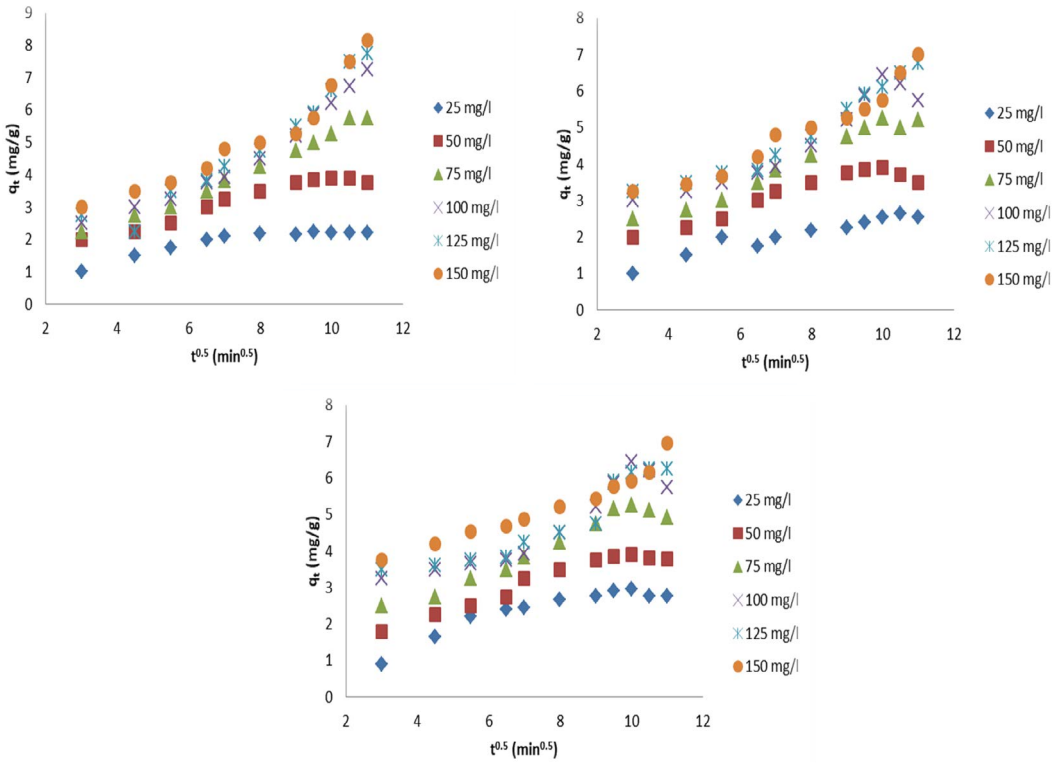

Fig. 13. IPD kinetic plots of Cr(VI), Pb(II), and Zn(II) metal ions.

Table 7
Isotherm constants for the removal of heavy metal ions by sugarcane bagasse

Isotherm model	Metal ion solution			
	Parameters	Cr(VI)	Pb(II)	Zn(II)
Langmuir	q_{max} (mg/g)	8.304	8.992	9.344
	K_L (L/mg)	0.334	0.147	0.104
	R^2	0.9715	0.9982	0.9866
Freundlich	K_f ((mg/g) (L/mg)$^{1/n}$)	2.514	1.823	1.399
	n (g/L)	2.936	2.351	2.062
	R^2	0.9508	0.9785	0.9400

studied with different heavy metal ions with sugarcane bagasse powder, for Cr(VI): Langmuir > Freundlich isotherm, for Pb(II): Langmuir > Freundlich isotherm, for Zn(II): Langmuir > Freundlich isotherm.

Referring to regression coefficient (R^2) values, adsorption of metal ions using sugarcane bagasse powder was fitted well with Langmuir isotherm model, than by Freundlich isotherm model. This is established on adsorption of metal ions by bagasse in the monolayer [9]. Based on the above observations, metal ions adsorption with the adsorbent follows heterogeneous and monolayer adsorption mechanism [43].

3.10. Impact of temperature and thermodynamic studies

The impact of temperature on metal ion removal has been investigated at different temperatures (15°C, 30°C, 45°C, and 60°C) and represented in Fig. 16, which indicates the importance of temperature in the adsorption process. At 20°C, the maximum efficiency rate was attained and after that, a gradual decrease in metal ion removal were identified with an increase in temperature. This may suggest that adsorption process between the adsorbent and heavy metal ions is an exothermic process and this was mainly due to a decrease in the active sites [44]. The values of $\Delta H°$ and $\Delta S°$ were determined from the slope and intercept of the plot of $\log K_c$ vs. $1/T$ as shown in Fig. 17. Table 8 indicates the values of $\Delta G°$, $\Delta H°$, and $\Delta S°$ in different temperatures along with varying initial concentrations (25–150 mg/L) of heavy metal ions (Cr, Pb, and Zn). From the table, negative $\Delta G°$ values with positive $\Delta H°$ indicate the performance of metal ions with sugarcane bagasse powder and the spontaneous nature of adsorption. From the above discussion, it was observed that the adsorption reaction follows endothermic nature [45]. Furthermore, the positive value of $\Delta S°$ suggests the increases in the uncertainty of solid/liquid interface at the time of metal ions adsorption on sugarcane bagasse powder in the aqueous medium.

4. Conclusion

The performance of biosorption of heavy metal ions (Cr, Pb, and Zn) was investigated using sugarcane bagasse powder in the batch adsorption process. By varying the metal ion concentration, pH of the solution, contact time, adsorbent dosage level, and temperature, the impact of adsorption efficiency were investigated. From batch studies, it was observed that the adsorption of metal ions onto adsorbent was increased with an increase in contact time and adsorbent dosage level. On the other hand, the process

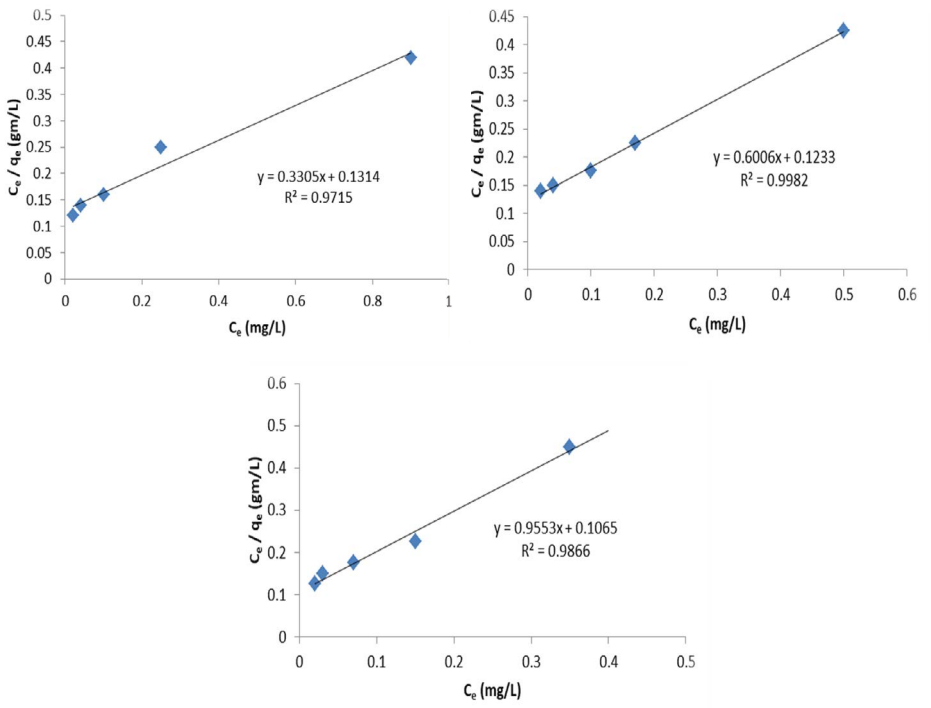

Fig. 14. Langmuir isotherm plots of Cr(VI), Pb(II), and Zn(II) metal ions.

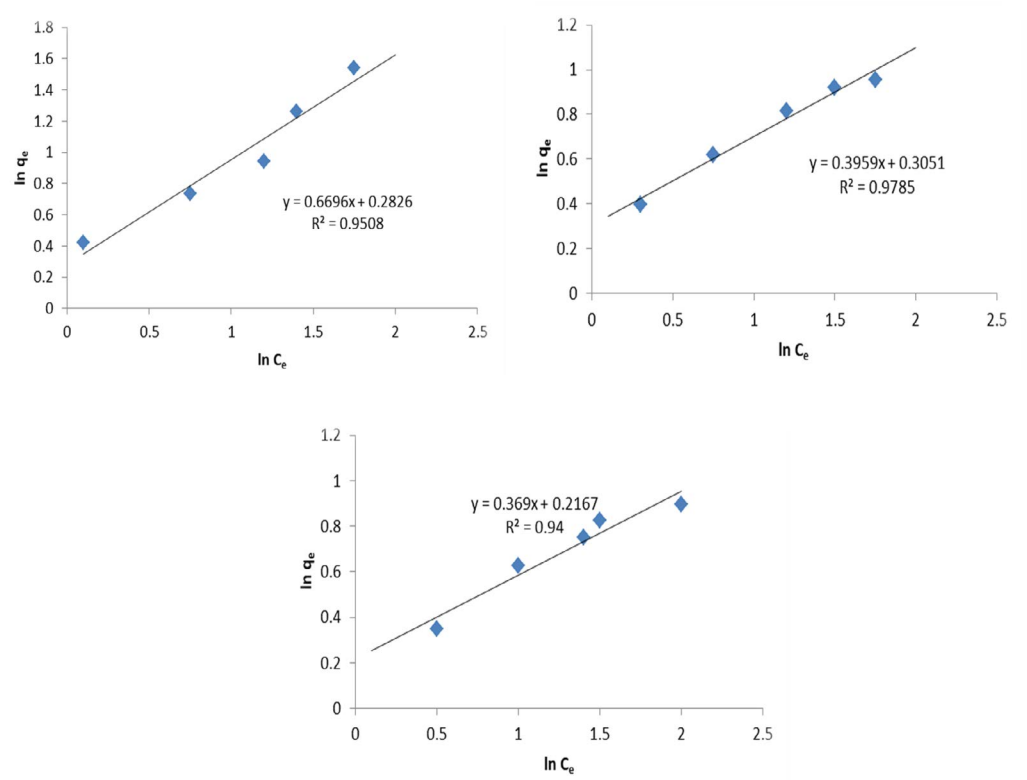

Fig. 15. Freundlich isotherm plots of Cr(VI), Pb(II), and Zn(II) metal ions.

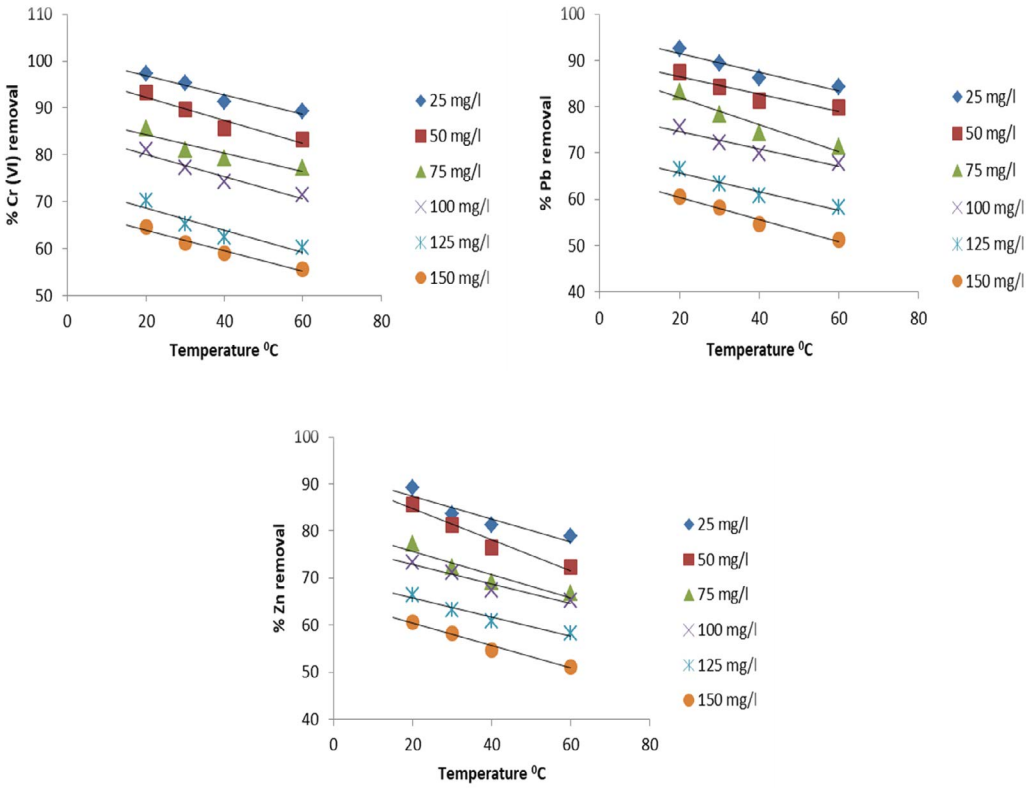

Fig. 16. Effect of temperature on the adsorption Cr(VI), Pb(II), and Zn(II) ions by SBP (initial ion concentration = 25–150 mg/L, dose = 1.2 g/L, pH = 6.0, and time = 60 min).

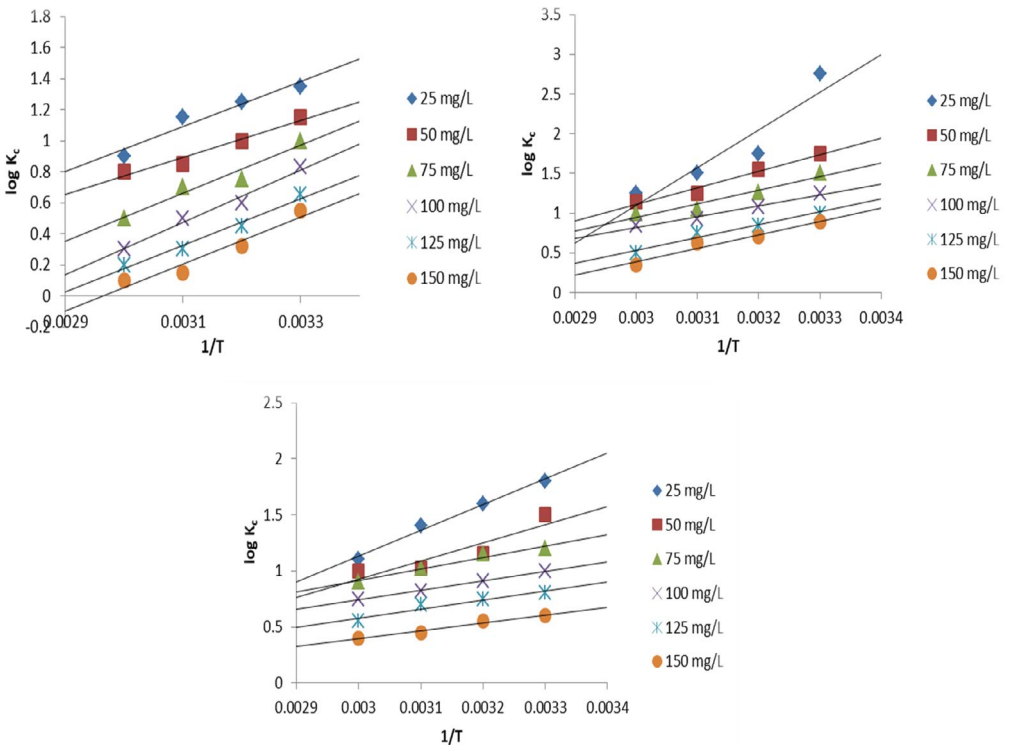

Fig. 17. Thermodynamic plots for the adsorption of Cr(VI), Pb(II), and Zn(II) ions using SBP.

Table 8
Thermodynamic parameters for the adsorption of metal ions using sugarcane bagasse

Initial ion concentration of Cr(VI) ions	$\Delta H°$ (kJ/mol)	$\Delta S°$ (J/mol)	$\Delta G°$ (kJ/mol)			
			15°C	30°C	45°C	60°C
25	32.764	80.723	–8.299	–7.587	–7.116	–6.942
50	20.134	42.542	–6.396	–6.244	–6.102	–5.632
75	18.678	36.923	–5.809	–5.568	–5.314	–3.449
100	13.452	25.766	–5.079	–3.888	–3.637	–3.135
125	11.823	21.145	–3.233	–3.214	–3.924	–3.752
150	9.345	19.623	–3.921	–3.786	–3.582	–3.245
Initial ion concentration of Pb(II) ions						
25	19.277	45.892	–6.810	–5.563	–5.238	–3.381
50	13.723	27.922	–3.892	–3.528	–3.347	–3.082
75	10.984	21.114	–3.962	–3.153	–3.196	–3.080
100	9.823	22.276	–2.183	–2.160	–2.377	–2.119
125	7.546	20.091	–1.182	–1.363	–1.246	–1.204
150	5.984	18.472	–0.892	–0.817	–0.820	–0.798
Initial ion concentration of Zn(II) ions						
25	13.376	28.491	–5.807	–3.671	–3.398	–3.162
50	11.036	23.881	–3.099	–3.484	–3.425	–3.298
75	9.311	20.392	–3.154	–2.920	–2.771	–2.458
100	8.741	21.923	–2.283	–2.056	–1.845	–1.648
125	7.293	18.467	–1.957	–1.414	–1.265	–1.029
150	6.756	16.873	–1.458	–1.037	–1.004	–1.036

of metal ion adsorption was decreased with an increase in solution's pH, the concentration of the adsorbate, and changes in temperature. The Langmuir and Freundlich isotherms fitted with the equilibrium data and pseudo-second-order kinetic model data has been followed in this adsorption process. From the above discussions, this work concluded that the sugarcane bagasse powder is the most efficient adsorbent to remove the heavy metal contaminations from the aqueous solutions.

References

[1] Y.S. Ho, Critical review of Lagergren kinetic rate equation on adsorption reactions, Scientometrics, 59 (2004) 171–177.

[2] A. Ali, K. Saeed, F. Mabood, Removal of chromium(VI) from aqueous medium using chemically modified banana peels as efficient low cost adsorbent, Alexandria Eng. J., 55 (2015) 2933–2942.

[3] S.S. Kalaivani, T. Vidhyadevi, A. Murugesan, K.V Thiruvengadaravi, D. Anuradha, S. Sivanesan, The use of new modified poly(acrylamide) chelating resin with pendent benzothiazole groups containing donor atoms in the removal of heavy metal ions from aqueous solutions, Water Res. India, 5 (2015) 21–35.

[4] I. Nirmala, Use of iron oxide magnetic nano adsorbents for Cr(VI) removal from aqueous solutions: a review, Int. J. Eng. Res. Appl., 4 (2014) 55–63.

[5] M.H. Kalavathy, T. Karthikeyan, S. Rajgopal, L.R. Miranda, Kinetic and isotherm studies of Cu(II) adsorption onto HPO-activated rubber wood sawdust, J. Colloid Interface Sci., 292 (2014) 354–362.

[6] J. Thilagan, A. Vimalkumar, K. Rajasekaran, C. Raja, Continuous fixed bed column adsorption of copper(II) ions from aqueous solution by calcium carbonate, Int. J. Eng. Res. Technol., 4 (2015) 413–418.

[7] B. Mao, A. Tok, S. Anyata, Removal of Lead Ion from Industrial wastewaters by activated carbon prepared from periwinkle shells (*Typanotonus fuscatus*), Turk. J. Eng. Environ. Sci., 31 (2007) 251–263.

[8] F. Boudrahem, F.A. Benissad, A. Soualah, Adsorption of Lead(II) from aqueous solution by using leaves of date trees as an adsorbent, J. Chem. Eng. Data, 56 (2011) 1804–1812.

[9] M. Vishnu, G. Niharika, B. Rajmohan, R. Keyur, Batch and continuous studies on the removal of heavy metals from aqueous solution using biosynthesised melanin-coated PVDF membranes, Environ. Sci. Pollut. Res., 27 (2020) 24723–24737.

[10] M. Jain, V. Kumar, K. Kadirvelu, Removal of Ni(II) from aqueous system by chemically modified sunflower biomass, Desal. Water Treat., 52 (2013) 5681–5695.

[11] T.T. Pham, M.T. Hoang, M.K. Nguyen, T.H. Dinh, P.L. Han, B.V. Bruggen, Evaluation of chemical modified sugarcane bagasse for cadmium removal in aqueous environment, Int. Proc. Chem. Biol. Environ. Eng., 88 (2015) 6–10.

[12] Y.J. Gao, Removal of cadmium and cobalt from heavy metal solution using oyster shells adsorbent, Asian J. Chem., 25 (2013) 8537–8540.

[13] K. Priyanka, Application of sugarcane bagasse for the removal of chromium(VI) and zinc(II) from aqueous solution, Int. Res. J. Eng. Technol., 4 (2017) 1670–1673.

[14] R. Kamal, S. Mitali, L. Nilesh, Adsorption of copper (Cu^{2+}) metal ion from wastewater using sulphuric acid treated sugarcane bagasse as adsorbent, Int. J. Adv. Eng. Res. Sci., 1 (2014) 55–59.

[15] C. Jiao, Y. Cheng, W. Fan, J. Li, Synthesis of agar–stabilized nanoscale zero valent iron particles and removal study of hexavalent chromium, Int. J. Environ. Sci. Technol., 12 (2012) 1603–1612.

[16] A.M. Nadeem, S.A. Mohammad, S.S. Shahid, A.M. Shah, G. Khalid, Sorption of lead from aqueous solution by chemically modified carbon adsorbents, J. Hazard. Mater., 138 (2006) 604–613.

[17] N. Kazem, N. Ramin, S. Reza, A.H. Mahvi, V. Forough, Y. Kamyar, G. Azar, N. Shahrokh, Biosorption of lead(II) and cadmium(II) by protonated sargassum glaucescens biomass in a continious packed bed column, J. Hazard. Mater., 147 (2007) 785–791.

[18] Q. Li, W. Zhai, W. Zhang, M. Wang, J. Zhou, Kinetic studies of adsorption of Pb(II), Cr(III) and Cu(II) from aqueous solution by sawdust and modified peanut husk, J. Hazard. Mater., 141 (2006) 163–167.

[19] H. Jing, H. Song, Z. Liang, G. Fuxing, H.Y. Shan, Equilibrium and thermodynamic parameters of adsorption of methylene blue onto rectorite, Fresenius Environ. Bull., 19 (2010) 2651–2656.

[20] P. Senthilkumar, H. Ethiraj, V. Anitha, N. Deepika, S. Nivedha, T. Vidhyadevi, L. Ravikumar, S. Sivanesan, Adsorption, kinetic, equilibrium and thermodynamic investigations of Zn(II) and Ni(II) ions removal by poly(azomethinethioamide) resin with pendent chlorobenzylidine ring, Pol. J. Chem. Technol., 3 (2017) 100–109.

[21] B. Agnes, N. Eliazar, O. Augustine, Intraparticle diffusion of Cr(VI) through biomass and magnetite coated biomass: a comparative kinetic and diffusion study, S. Afr. J. Chem. Eng., 32 (2020) 39–55.

[22] M.A. Ahmad, Kinetic equilibrium and thermodynamic studies of synthetic dye removal using pomegranate peel activated carbon prepared by microwave–induced KOH activation, Water Res. Ind., 06 (2014) 18–35.

[23] M. Xiaojun, Y. Hongmei, Y. Lili, C. Yin, L. Ying, Preparation, surface and pore structure of high surface area activated carbon fibers from bamboo by steam activation, Materials, 7 (2014) 4431–4441.

[24] N.S. Langeroodi, Z. Farhadravesh, A.D. Khalaji, Optimization of adsorption parameters for Fe(III) ions removal from aqueous solutions by transition metal oxide nanocomposite, Green Chem. Lett. Rev., 11 (2018) 404–413.

[25] H.N.M.E. Mahmud, A.O. Huq, R. Binti, The removal of heavy metal ions from wastewater/aqueous solution using polypyrrole-based adsorbents: a review, RSC Adv., 06 (2016) 14778–14791.

[26] T. Vidhyadevi, A. Murugesan, S.S. Kalaivani, M.P. Premkumar, V. Vinothkumar, L. Ravikumar, Evaluation of equilibrium, kinetic, and thermodynamic parameters for adsorption of Cd^{2+} ion and methyl red dye onto amorphous poly(azomethinethioamide) resin, Desal. Water Treat., 52 (2014) 3477–3488.

[27] W.J. Weber, J.C. Morris, Kinetics adsorption on carbon from solutions, J. Sanitary Eng. Div., 89 (1963) 31–60.

[28] N. Zulfareen, T. Venugopal, I. Sajitha, Removal of zinc from synthetic wastewater by activated carbon propsopis juliflora, Int. J. Adv. Sci. Eng., 4 (2018) 746–749.

[29] O.O. Ogunleye, M.A. Ajala, S.E. Agarry, Evaluation of biosorptive capacity of banana (*Musa paradisiaca*) stalk for lead(II) removal from aqueous solution, J. Environ. Prot., 05 (2014) 1451–1465.

[30] O. Joseph, M. Rouez, H.M. Pignon, B. Remy, E. Evens, G. Remy, Adsorption of heavy metals on to sugarcane bagasse: improvement of adsorption capacities due to anaerobic degradation of the biosorbent, Environ. Technol., 30 (2009) 1371–1379.

[31] T. Sathish, N.V. Vinithkumar, G. Dharani, R. Kirubagaran, Efficacy of mangrove leaf powder for bioremediation of chromium(VI) from aqueous solutions: kinetic and thermodynamic evaluation, Appl. Water Sci., 5 (2015) 153–160.

[32] R. Lakshmipathy, N.C. Sarada, A fixed bed column study for the removal of Pb^{2+} ions by watermelon rind, Water Res. Technol., 1 (2015) 244–250.

[33] Y.S. Ho, G. Mckay, Pesudo-second-order model for sorption process, Process Biochem., 34 (1999) 451–465.

[34] F. Qin, B. Wen, X.Q. Shan, Y.N. Xie, Mechanisms of competitive adsorption of Pb, Cu and Cd on peat, Environ. Pollut., 144 (2015) 669–680.

[35] P. Senthil Kumar, S. Ramalingam, V. Sathyaselvabala, S. Dinesh Kirupha, A. Murugesan, S. Sivanesan, Removal of cadmium(II) from aqueous solution by agricultural waste cashew nut shell, Korean J. Chem. Eng., 29 (2012) 756–768.

[36] M.T. Amin, A.A. Alazba, M. Shafiq, Batch and fixed bed column studies for the biosorption of Cu(II) and Pb(II) by raw and treated date palm leaves and orange peel, Global Nest J., 19 (2017) 464–478.
[37] H.A. Hegazi, Removal of heavy metals from wastewater using agricultural and industrial wastes as adsorbents, HRBC J., 9 (2013) 276–282.
[38] A.K. Priya, S. Nagan, M. Nithya, P.M. Priyanka, M. Rajeswari, Assessment of tendu leaf refuses for the heavy metal removal from electroplating effluent, J. Pure Appl. Microbiol., 10 (2016) 585–591.
[39] W. Kong, J. Ren, S. Wang, Q. Chen, Removal of heavy metals from aqueous solutions using acrylic-modified sugarcane bagasse based adsorbents: equilibrium and kinetic studies, BioResources, 9 (2014) 3184–3196.
[40] N.Y. Yarkandi, Removal of lead(II) from waste water by adsorption, Int. J. Curr. Microbiol. Appl. Sci., 3 (2014) 207–228.
[41] V. Yogeshwaran, A.K. Priya, Removal of heavy metals using nano particles – a review, Ind. J. Environ. Prot., 39 (2019) 17–21.
[42] T.V. Tran, Q.T. Phoung, T.D. Nguyen, N.T. Hong le, L.G. Bach, A comparative study on the removal efficiency of metal ions (Cu^{2+}, Ni^{2+} and Pb^{2+}) using sugarcane bagasse derived $Zncl_2$ – activated carbon by the response surface methodology, Adsorpt. Sci. Technol., 35 (2017) 72–85.
[43] S.M.E. Yakout, A.A. Abdeltawab, K. Elhindi, A. Askalany, Uranium dynamic adsorption breakthrough curve onto rice straw based activated carbon using bed depth service time model, BioResources, 13 (2018) 9143–9157.
[44] H.D.S.S. Karunarathne, B.M.W.P.K. Amarasinghe, Fixed bed adsorption column studies for the removal of aqueous phenol from activated carbon prepared from sugarcane bagasse, Energy Procedia, 34 (2013) 83–90.
[45] M.M. Saeed, A. Munir, Effect of temperature on kinetics and adsorption profile of endothermic chemisorption process: – Tm(III) – PAN loaded PUF system, Sep. Sci. Technol., 41 (2005) 705–722.